JTTEE5 19:611–619
DOI: 10.1007/s11666-009-9459-2
1059-9630/$19.00 © ASM International

Grindability Evaluation and Fatigue and Wear Behavior of Conventional and Nanostructured Al_2O_3-13 Wt.% TiO_2 Air Plasma Sprayed Coatings

M. Ramazani, J. Khalil-Allafi, and R. Mozaffarinia

(Submitted June 13, 2009; in revised form September 18, 2009)

In this paper, air plasma spray Al_2O_3-13% TiO_2 coatings were produced by two type of feedstock powders (agglomerated nanostructured and conventional). Mechanical properties of coatings including hardness, toughness, fatigue, and wear behavior as well as grindability of coatings were evaluated and compared. We report that due to the presence of nanostructure zone in microstructure of air plasma sprayed Al_2O_3-13% TiO_2 nanostructure coatings, a significant gain is observed in toughness, grindability, and fatigue lifetime in nanostructure coating over its counterpart conventional coating.

Keywords air plasma spray, Al_2O_3-13% TiO_2, fatigue, grindability, nanostructure coating, toughness

1. Introduction

Nanostructure ceramic coatings currently open a wide range of research opportunities for nanoceramic materials. Recently, there has been a growing interest in producing nanostructure ceramic coatings by thermal spray processes. Air plasma spray technique has been employed as a production method for nanostructure ceramic coatings due to its higher working temperature in comparison to other thermal spray processes (Ref 1). Thermal spray ceramic coatings are usually made from a powder feedstock. These powder particles *typically* exhibit a particle size distribution varying from 5 to 100 μm, i.e., the particles are microscopic. Fine particles, including nanosized particles, i.e., smaller than 100 nm, cannot be thermal sprayed using the regular powder feeders currently being employed in thermal spray. However, plasma spray process of nano-powders is more complicated than conventional powders. The nano-powders do not have enough momentum in plasma spraying and therefore cannot inject them into the plasma jet directly. Nanoparticles should be agglomerated into sprayable agglomerated particles with sprayable diameter *typically* 5-100 μm (i.e., microscopic size) or in other method (in Solution Precursor Plasma Spray Processing method) injected by suspension (Ref 2-6). In plasma spraying of nanostructured agglomerated powders, the microstructure and properties of nanostructure coatings could be related to an empirical parameter that is defined as the critical plasma spray parameter (CPSP). CPSP is calculated with Eq 1 where V is plasma voltage (volt), A is plasma current intensity (ampere), and the denominator in the equation is plasma gas flow (in standard cubic foot per hour) (Ref 4-6).

$$\mathrm{CPSP} = \frac{V \times A}{\text{plasma gass flow (SCFH)}}. \qquad \text{(Eq 1)}$$

CPSP has a direct effect on plasma temperature, and an increase in this parameter causes an increase in plasma temperature. Microstructure and properties of nanostructure coatings can be controlled by modification of CPSP (Ref 3, 5, 6).

Anti-wear thermal spray coatings produced from nanostructured ceramic agglomerated powders are currently in use on parts employed by the U.S. Navy (Ref 7). The choice of a nanostructured material for anti-wear applications was based on knowledge gained in developmental work (Ref 8-13). The specific application involves the use of APS nanostructured Al_2O_3-13% TiO_2 coatings applied on the main propulsion shaft of ships. These shafts suffered from severe abrasion on the bearing surfaces, causing frequent and costly repairs. The use of conventional ceramic coatings was not considered feasible due to the high levels of torque, bending, and fatigue experienced by these pieces, which normally would lead to failure of these conventional thermal spray coatings. However, due its known high toughness, the nanostructured Al_2O_3-13 wt.% TiO_2 ceramic coating was applied on the propulsion shafts of several U.S. Navy ships. One of these ships was inspected for any signs of coating wear after 3 months in operation. No visual signs of wear were

M. Ramazani, Shand University of Technology, Tabriz, Iran and Malek Ashtar University of Technology, Shahin Shahr, Iran; **J. Khalil-Allafi**, Shand University of Technology, Tabriz, Iran; and **R. Mozaffarinia**, Malek Ashtar University of Technology, Shahin Shahr, Iran. Contact e-mail: mazaher.ramazani@gmail.com.

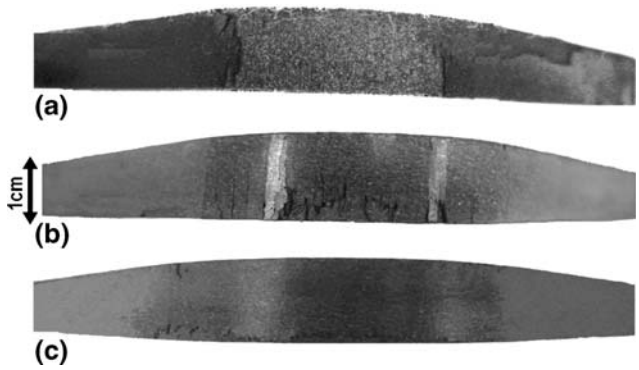

Fig. 1 Behavior of (a) conventional, (b) nonoptimized nanostructured, and (c) optimized nanostructured (CPSP = 393) coatings in bend test

detected. After 4 years in service, the ship was inspected again and no significant wear or delamination was recorded (Ref 13).

The effects of CPSP on microstructure and properties of the plasma sprayed coatings, including porosity, microhardness, adhesion, and toughness in bending tests were evaluated elsewhere (Ref 14). It was found that nanostructure Al_2O_3-13% TiO_2 coatings exhibit superior adhesion and toughness. Figure 1 shows different behavior of conventional coatings and optimized nanostructure (CPSP = 393) coatings in the bending test (optimized nanostructure coating is produced by suitable plasma spray parameter, CPSP = 393 this coating exhibit maximum adhesion and toughness). Toughness and adhesion in nanostructure coatings are better than conventional coatings. In fact, these investigations showed that toughness and adhesion of nanostructure coatings in all conditions are superior in comparison to conventional coatings (Ref 14). Measuring crack propagation resistance and evaluation of coating toughness were done on nanostructure and conventional coatings (Ref 14). The crack propagation resistance was determined by indenting the coating cross sections with a Vickers indenter at a 5 kgf load (50 N) for 15 s. The indenter was aligned so that one of its diagonals would be parallel to the substrate surface. The total length (tip-to-tip) of the major crack ($2c$) parallel to the substrate surface that originated at or near the corners of the Vickers indentation impression was measured. Based on the indentation load (P) and $2c$, the crack propagation resistance was calculated according to the relation between load and crack length $p/c^{3/2}$, where p is in Newton and c is in meters. Toughness of coating was calculated from Eq 2 where α is an empirical constant which depends on the geometry of the indenter, E is modulus of elasticity, and H is hardness of coating (Ref 14). Results showed that an increase in CPSP in plasma spray process leads to an increase in the hardness of nanostructure coatings (Ref 15-20). Nevertheless, the crack growth resistance and coating toughness initially increased with an increase in CPSP, and then decreased (Ref 15). This behavior is attributed to existence of the nanostructure zones which were embedded in the coating

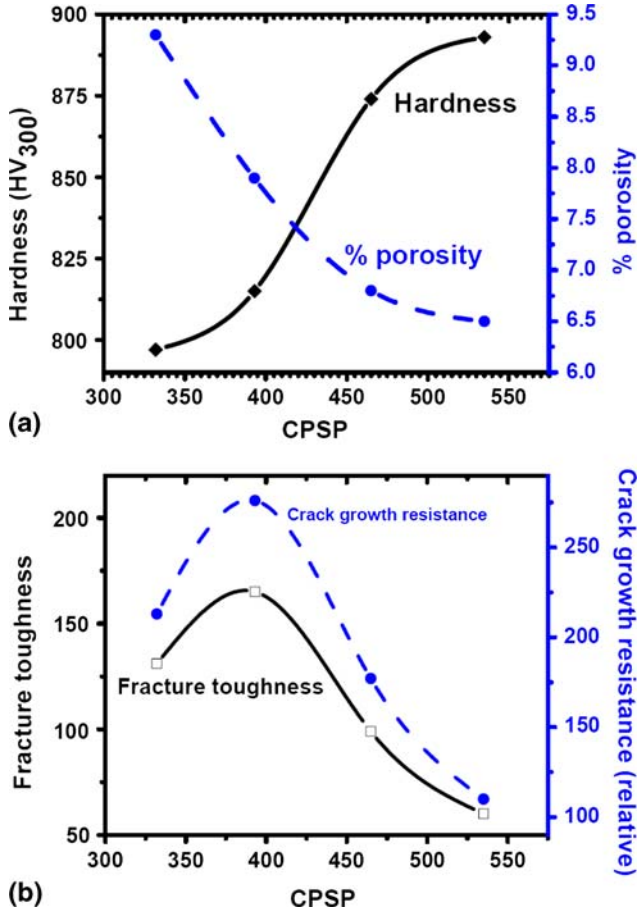

Fig. 2 Effect of CPSP on (a) porosity, hardness, and (b) crack growth resistance and toughness of nanostructured coatings

microstructure that act as crack arresters and assist to impede crack propagation (Ref 3, 5-7, 19, 20). Figure 2(a) and (b) summarizes some results of previous paper (Ref 13, 19) including the influence of CPSP on porosity, hardness, and crack growth resistance and toughness of nanostructure coatings. Figure 2(b) illustrates that nanostructure coating with the CPSP = 393 has optimized properties.

$$K_C = \alpha\left(\frac{E}{H}\right)^{1/2}\frac{P}{C^{3/2}}. \qquad \text{(Eq 2)}$$

Grindability is a numerical indication of capacity of a given material to be ground under given machining conditions. Extensive investigations for grindability of various technical ceramics in form of bulk and coating materials indicated that grindability is a crucial characteristic of ceramics that cannot be evaluated by common mechanical properties such as hardness, toughness and elastic modulus (Ref 21-24). However, it is necessary to develop ceramic coatings with superior mechanical properties as well as good grindability. In addition, evaluation of grindability gives insight in development of ceramic coating materials to realize the overall cost effectiveness of ceramic components.

Fatigue life and its mechanism are another important characteristic of APS ceramic coatings. Microstructure of APS coatings consists of splat boundaries and inter-splat porosities oriented in different directions. These porosities and cracks act as stress concentrated spots which lead to crack nucleation and/or crack growth under cyclic load. However, failure mechanism APS coating under fatigue is dominated by propagation of pre-existing microcracks to the coating/substrate interface followed by delamination of coating.

2. Experimental Procedures

The ceramic Al_2O_3-13% TiO_2 coatings were produced by air plasma spray technique using two different commercially available nanostructured agglomerated Al_2O_3-13% TiO_2 (spray dried Nanox™ s2613s) and conventional Al_2O_3-13% TiO_2 (METCO 130) feedstock powders. For comparison, the corresponding conventional coating was deposited with parameters recommended by the powder manufacturer. The plasma spraying was carried out with a Metco A-2000 atmospheric plasma spraying equipment (Sulzer Metco AG) with spraying distance 120 mm, number of torch passes 4, carrier gas flow rate (Ar) 3.5 slpm, plasma gas flow rate Ar = 41; H_2 = 14 slpm, cooling gas (Ar) 8.5 bar, and deposition temperature 70-150 °C. Substrate samples of 120 × 10 × 4 mm^3 were cut from low carbon steel. Prior to plasma spraying, substrate was grit-blasted with #36 alumina. The resulting average surface roughness was about 10 mm Ra. Different plasma spray parameters listed in Table 1 were used for deposition of coatings. Several processing parameters such as carrier gas flow rate, spray distance, flow rate ratio of Ar-to-H_2, powder feed rate, and gun traverse speed, were held constant.

The microstructure of the powder was analyzed with scanning electron microscopy (SEM) and x-ray diffraction (XRD).

For evaluation of grindability, coatings are ground under particular and constant conditions including constant force, wheel speed, etc., and the total time needed for grinding was measured and quality of ground surface as a result of tests was evaluated.

Grindability can be considered in terms of productivity, cost, and quality. The cost-effective machining of ceramics requires that measuring of grindability should be practically easy. Volumetric removal rate under controlled-force grinding is a cost-effective measurement of ceramic grindability (Ref 21-24). Under controlled-force grinding, material removal rate is a function of normal grinding force (F_n), wheel speed (v_s), material properties (ϕc), and wheel characteristics (ϕd). Material removal rate Z_w (volumetric material removal per unit time and unit width of grinding) can be expressed as:

$$Z_w = f(V_s, F_n, \phi c, \phi d). \quad \text{(Eq 3)}$$

If the same kind of diamond wheel is used for all the grindability tests, the influence of diamond wheel on material removal rate can be excluded from Eq 3. This is similar to hardness test in which some predetermined indenters should be used in order to obtain comparable results. Therefore, the material removal rate per unit normal grinding force is defined as the material removal parameter, or

$$\Delta_w = \frac{\partial Z_w}{\partial F_n}. \quad \text{(Eq 4)}$$

Under controlled-force grinding, material removal parameter Δ_w increases with wheel speed V_s. To find a parameter depending only on material properties, we define λ_w parameter

$$\lambda_w = \frac{\partial \Delta_w}{\partial V_s} = \frac{\partial}{\partial V_s}\left[\frac{\partial Z_w}{\partial F_n}\right], \quad \text{(Eq 5)}$$

where λ_w is volumetric material removal rate per unit wheel speed and unit normal grinding force. Proportional relationships exist between material removal rates and both wheel speed and normal force. Therefore, grindability $G(c)$ can be defined as (Ref 23)

$$G_c = \lambda_w = \frac{Z_w}{V_s F_n} = g(Q_c). \quad \text{(Eq 6)}$$

Due to the fact that ceramic grindability under constant wheel speed and grinding force depends only on material characteristics, evaluation of grindability was carried out in constant normal force and wheel speed. Ceramic volume loss was measured and quality of ground surface was evaluated by SEM. There is no available standard material for determining ceramics grindability, so in practice grindability should be reported comparative and relative.

Grinding parameter and conditions in grindability evaluation of this research were selected similar to industrial grinding condition. TBN wheel, wheel speed 3000 rpm, and 8 mm/s traverse speed were used. A constant compressive load is applied to the specimen, grinding is performed in a 30-s cycle, and the specimen volume loss is measured at the end of the cycle. Grindability evaluation was performed by the comparability study of the rate of material removal (volume loss rate) in grindability test and quality of ground surfaces (roughness, cracking, chipping, delamination, etc.).

The fatigue behavior and grindability properties of these coatings were comparatively investigated. Cyclic tensile (bending) fatigue was conducted at room temperature to simulate the loading condition in which coating materials will be exposed to tensile stress in service condition. Fatigue behavior was evaluated from cyclic bending tests at room temperatures and cyclic frequency in fatigue test was 1 Hz. Specimens have been exposed to

Table 1 Plasma spraying parameters used in the study

No.	CPSP	Current, A	Voltage, V	Powder type	Designation
1	286	350	72.5	Nanostructured	NS286
2	332	400	71.5	Nanostructured	NS332
3	357	450	70	Nanostructured	NS357
4	393	500	69	Nanostructured	NS393
5	427	550	68.3	Nanostructured	NS427
6	480[a]	600	69.5	Conventional	CC480

[a]This the parameters recommended by the powder manufacturer

cyclic bending fatigue in strain-controlled mode. The test specimen used in the fatigue tests was 120 × 4 × 20 mm^3 plates and coatings thickness was 250 μm. The fatigue experiments were performed at room temperature. Formation and growth of cracks in coating and coating/interface were examined after each 1000 cycle using an optical microscope during test experiment, and SEM. The number of applied cycles that leads to obvious cracks on the coating surface was registered.

Wear tests were carried out by pin on plate wear test machine at room temperature. DIN 100Cr6 standard pin was used for testing. Before wear test, samples were ground up to 250 μm coating thickness. First, the loadability test was performed on conventional and optimized nanostructured (CPSP = 393) coating samples. Then, coatings were exposed to wear test with 24 kg (240 N) load and 1000 m sliding distance. The sliding speed during the wear test was 0.2 m/s. In wear test, the volume loss of specimen was measured after a different sliding distance. In loadability test, after each 100 m sliding distance volume loss of specimen was measured and then in the further step of loadability test (further 100 m) load 3 kg (30 N) was increased. Namely, in loadability test the load were increased staircase (with 3 kg of increase in each step) after measuring the volume loss of specimens in each step, until loadability limit of specimen obtained. Furthermore in each test pin weight loss was also measured.

Coating wear surface and wear cross section of the coatings was evaluated by SEM to determine wear mechanism.

3. Results and Discussion

Scanning electron microscope image of the morphology of conventional and agglomerated Al_2O_3-13% TiO_2 powders are shown in Fig. 3(a) and (b). Figure 3(c) shows agglomerated powders with higher magnification that illustrates nanostructure of this powder. Each microscopic agglomerated feedstock particle is formed by agglomeration via spray-drying of several individual nanosize particles of alumina and titania with 13 wt.% TiO_2.

Microstructures of conventional and nanostructure coatings cross section are shown in Fig. 4. The nanostructure coatings show two distinct microstructure features. Coating made by nanostructure powder shows two regions, fully melted and partially melted. In the partially melted region, we obtained nanostructure similar to the one in the starting powder feedstock. On the other hand, in fully melted region there was no evidence of nanostructures. Nevertheless conventional coating has a splat lamellar morphology (only full melted regions). It has been shown that regions with nanostructure coatings act as crack arrester in coating and cause an increase in relative fracture toughness and crack growth resistance of nanostructured coatings (Ref 19).

The material removal (volume loss) diagrams for optimized nanostructured coating and conventional coatings in grindability evaluation test are presented in Fig. 5.

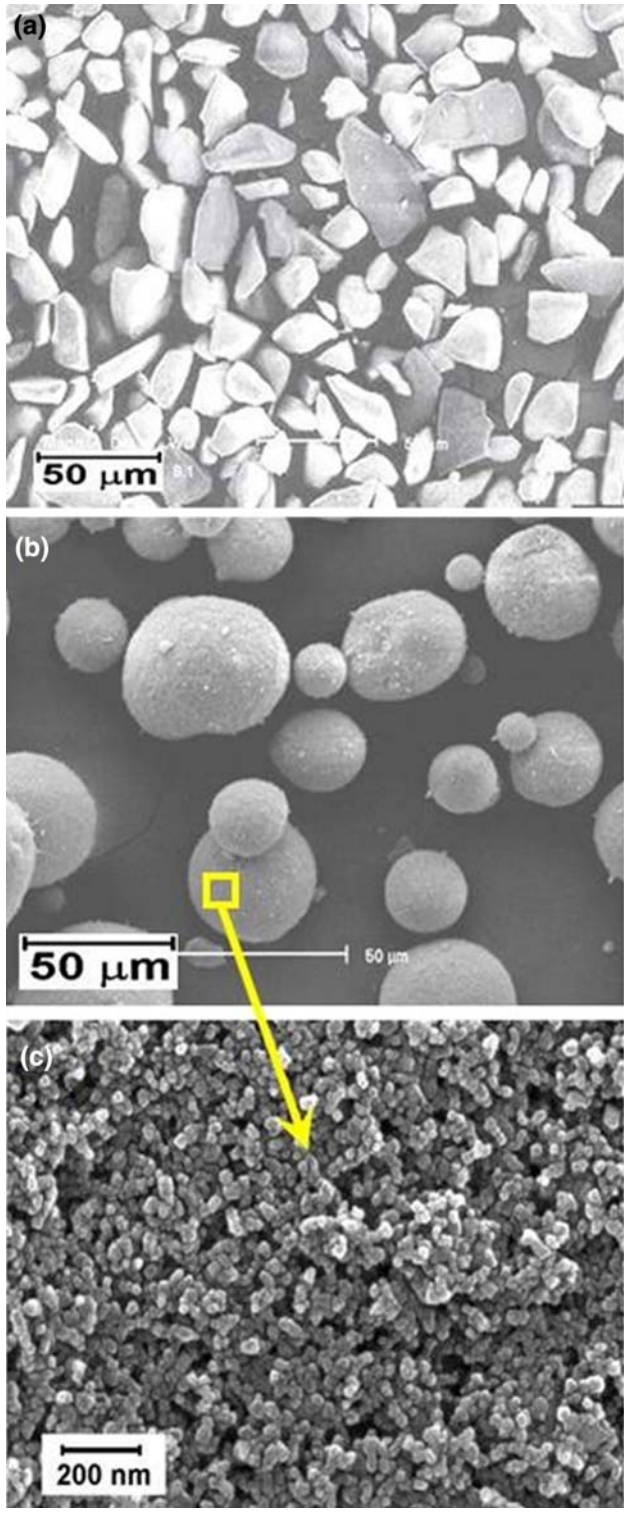

Fig. 3 Scanning electron microscope images of (a) conventional and (b and c) agglomerated Al_2O_3-13% TiO_2 powders

The material removal in grinding test for conventional coating is clearly lower than nanostructured coatings. The rate of material removal in grinding test conditions is 1.2 and 0.7 (10^3 cm^3/s) for nanostructure and conventional

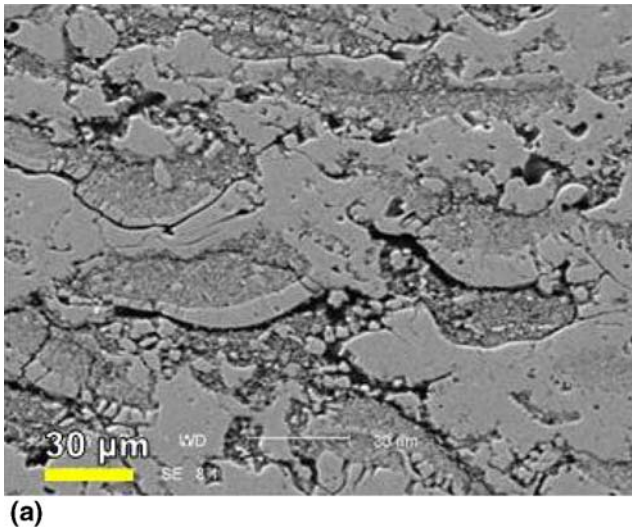

Fig. 4 SEM images of (a) nanostructured and (b) conventional coatings cross sections

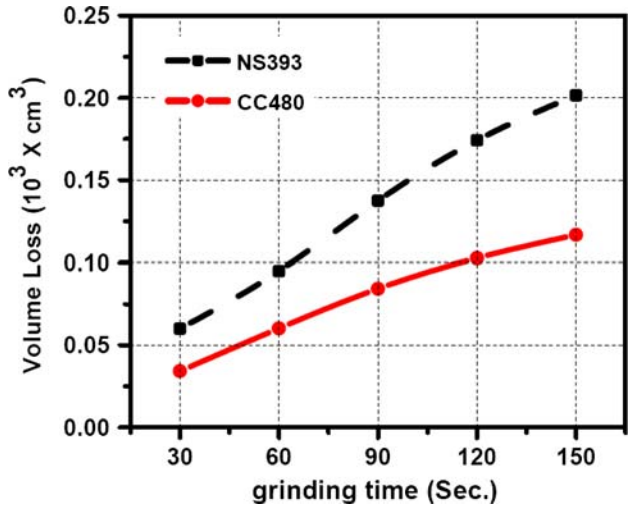

Fig. 5 Material removal (volume loss) diagrams for optimized nanostructured coating (CPSP = 393) and conventional coatings in grindability evaluation test

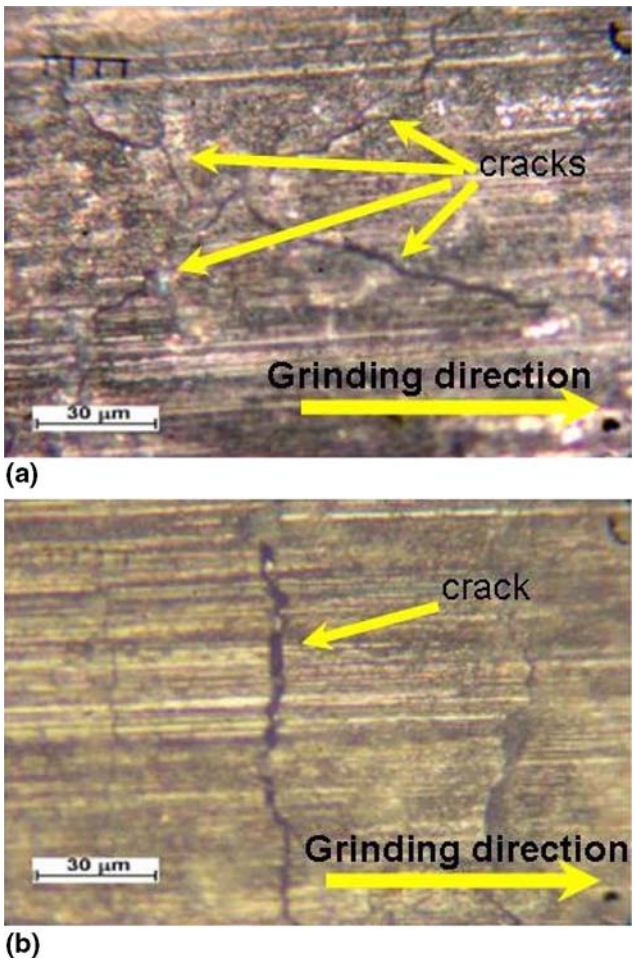

Fig. 6 Typically cracks in ground surfaces of (a) conventional and (b) nanostructured coatings

coatings, respectively. Thus, grindability (according to volumetric material removal rate) on nanostructured coating is better than conventional coatings. Figure 6 showed typical cracks produced in ground surface of samples during grinding. Our investigations show that a few large cracks in grinding directions were observed on the conventional coating which were perpendicular to the grinding direction, while a lot of small cracks in all directions (approximately isotropic) were observed on the nanostructured coating ground surface (Fig. 5). Furthermore, surface roughness of ground conventional and nanostructured coatings were 1.5 and 0.5 µm, respectively. The surface roughness of the ground surface of the test specimens correlate directly with the grindability of coating and reflects another attribute of grindability of material or the ability of a material to be ground smoothly without leaving excessive rough and pitted areas. So (a) nanostructured coatings can be ground approximately

in half the time required for conventional coatings, while (b) the nanostructure coating surface is more smoothly than conventional coating, and (c) in these grinding conditions the produced cracks on the conventional coating surface are worse than nanostructure coating (Fig. 6). In conclusion, the grindability of the nanostructured coating (grinding quality and rate) is more than that in conventional coating. Higher relative toughness and crack growth resistance and homogeneous structure of the nanostructured coating are the estimated origins for increasing grindability of nanostructured coatings.

Conventional and nanostructured coating fatigue lifetime is illustrated in Fig. 7. Figure 8 and 9 shows typical images of coating/substrate interface cross sections and cracks in coating surface in nanostructure (after 10^7 cycle) and conventional (after 10^6 fatigue cycles) coatings. In fatigue testing, extensive delaminating was not found in nanostructured coating after 10^7 cycle (only microcracks were observed), while full delamination was found in conventional coating after 10^6 cycle. Also delamination was not found anywhere in nanostructured coating/substrate interface after 10^7 cycle. Fatigue cracks in conventional coatings will emanate from the coating/substrate interface, while in nanostructured coatings cracks will emanate in both coating and coating/substrate interface. During fatigue test, cracks will grow from pores and microcracks. Thus, pores and microcracks in the coating material serve as areas of stress concentration.

Loadability test results prepared in present research for the conventional and optimized nanostructured coatings (CPSP = 393) are shown in Fig. 10. Figure 11 shows volume loss diagrams of the nanostructured and conventional coatings. Based on the volume loss diagrams, the wear rate of each coating is calculated (in cm^3/m) and is presented in Fig. 12 in the form of wear rate diagram versus CPSP. The volume loss diagram of sliding wear tests for both samples is shown in Fig. 13. SEM images of conventional and nanostructure coating wear surface is illustrated in Fig. 14 and 15 presents SEM images of the worn surfaces cross section of the nanostructured and conventional coatings.

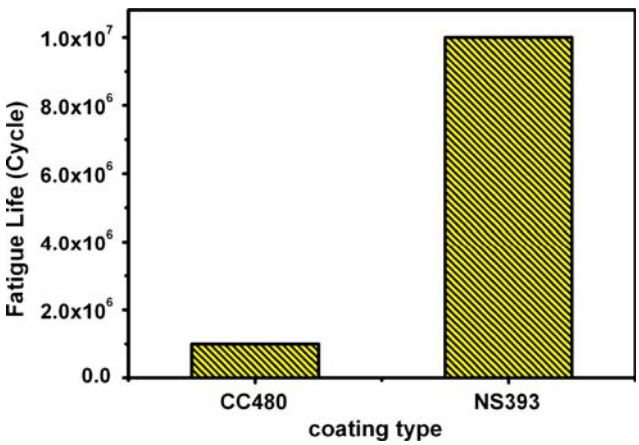

Fig. 7 Conventional and nanostructured coating fatigue lifetime

The higher crack growth resistance in nanostructured coatings during fatigue tests cause the cracks arresting in semi-melted (nanostructured) regions of the nanostructured coating, but in conventional coatings the fatigue cracks grow very fast and cause coatings to be useless (Ref 19).

Loadability is one of the important criteria and factors in selection of a coating, and based on Fig. 7 loadability in conventional coating is about 18 kg while in nanostructured coatings loadability is 30 kg (300 N), so the loadability of nanostructured coating is approximately twice as much as the loadability of the conventional coating.

By comparing Fig. 11 and 12, we can conclude that in all cases nanostructured coating wear resistance is more than conventional coating. Also an increase in CPSP leads to a decrease in wear rate in nanostructured coating (Fig. 11 and 12), whereas an increase in CPSP leads to an increase in nanostructured coating toughness (Fig. 2a and b). Therefore, we concluded an increase in nanostructured coating wear resistance due to an increase in CPSP is

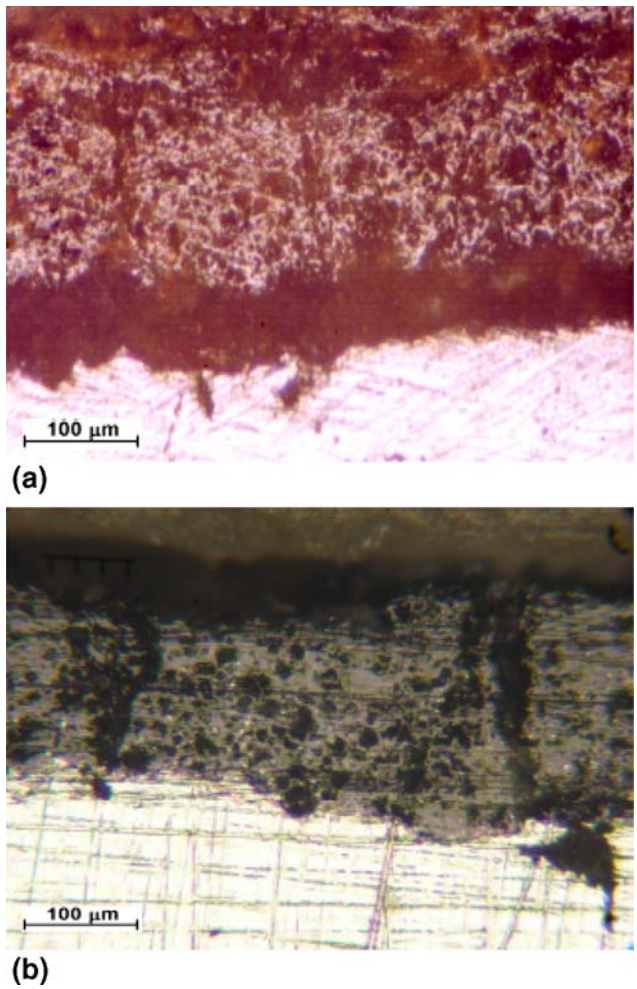

Fig. 8 Typically images of coating/substrate interface cracks in ground surfaces of nanostructured (after 10^7 cycle) and conventional (after 10^6 fatigue cycle) coatings

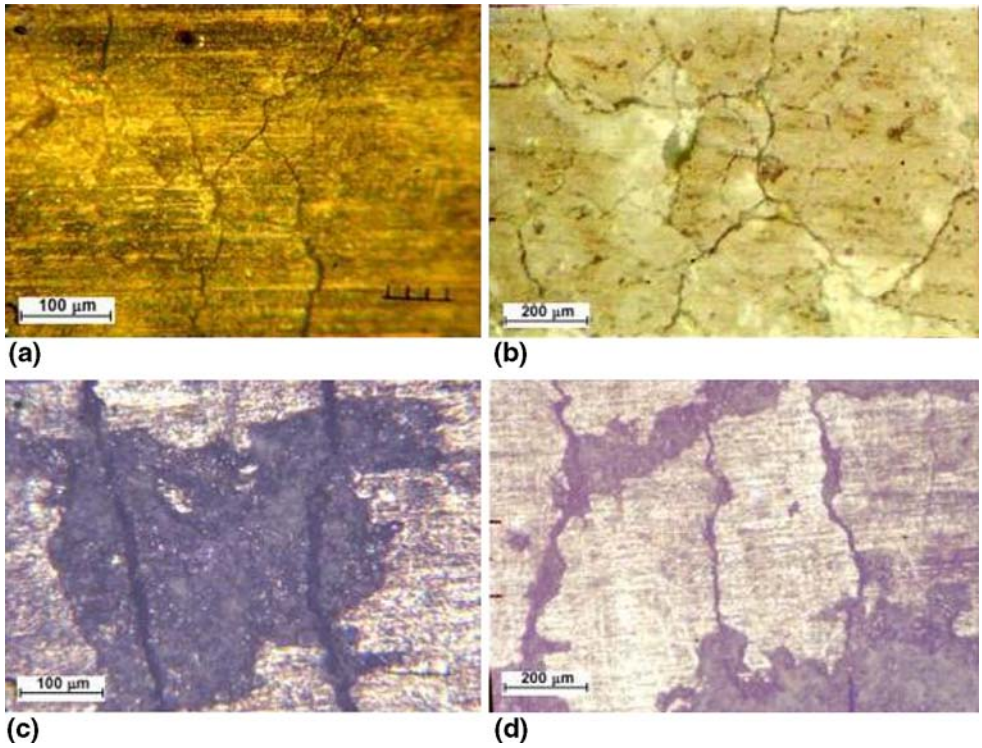

Fig. 9 Typically images of surface cracks in ground surfaces of the nanostructured (after 10^7 cycle) and conventional (after 10^6 fatigue cycle) coatings

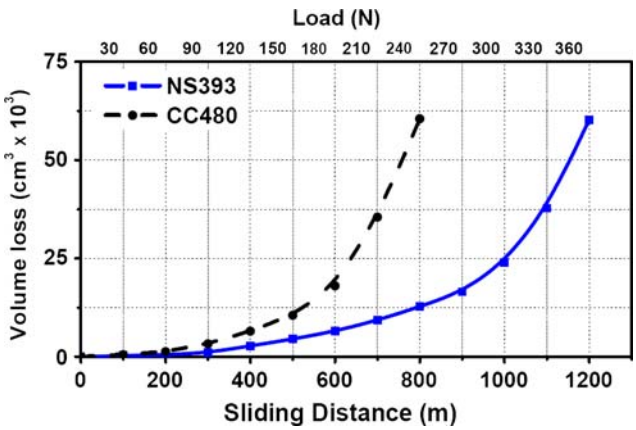

Fig. 10 Loadability test results of the conventional and optimized nanostructured (CPSP = 393) coatings

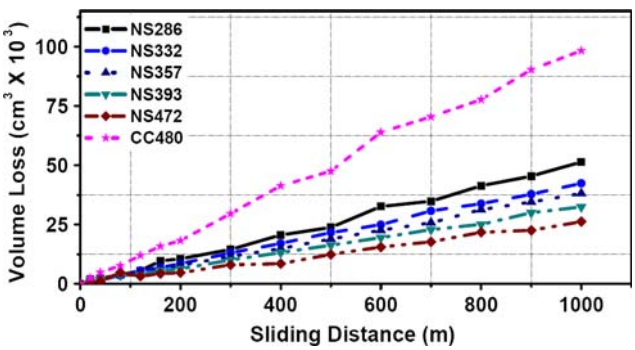

Fig. 11 Volume loss diagrams of the nanostructured and conventional coatings in pin on plate wear test

because of an increase in its toughness. By increasing CPSP, the pin wear (weight loss of pin) increased (Fig. 13) because of an increase in coating hardness (Fig. 2a).

Nanostructured coating wear rate is about a quarter of conventional coating (Fig. 12), so, wear resistance in nanostructured coating is about a fourfold conventional coating. For studying the origin of this difference, we compare the images of wear surface and cross section of the optimized (CPSP = 393) nanostructured and conventional coatings presented in Fig. 14 and 15.

Due to the existence of major cracks produced in wear surface of the conventional coating, the basic wear mechanism in conventional coating is brittle fracture. Wear surface of nanostructured coatings has very smooth features (Fig. 14) which are the characteristic of wear with plastic deformation mechanism, study and comparison of nanostructured and conventional coatings worn cross section are useful in understanding and detection of wear mechanisms of conventional and nanostructured coatings (Fig. 14 and 15). During wear test, numerous cracks were created in nanostructured coatings but because of the high crack growth resistance in this coatings, these cracks were quickly terminated, so in nanostructured coating worn

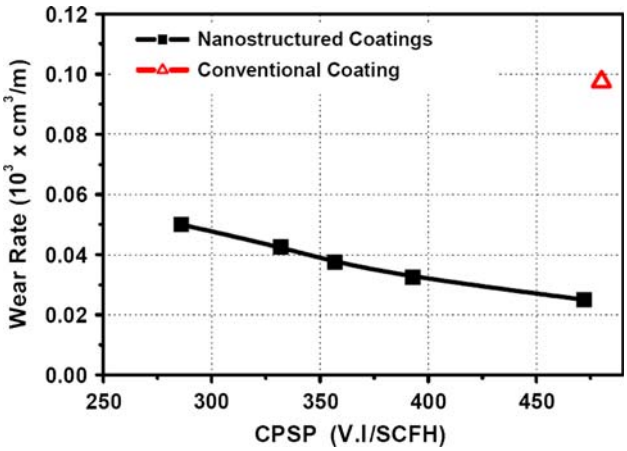

Fig. 12 Wear rate of nanostructured and conventional coatings

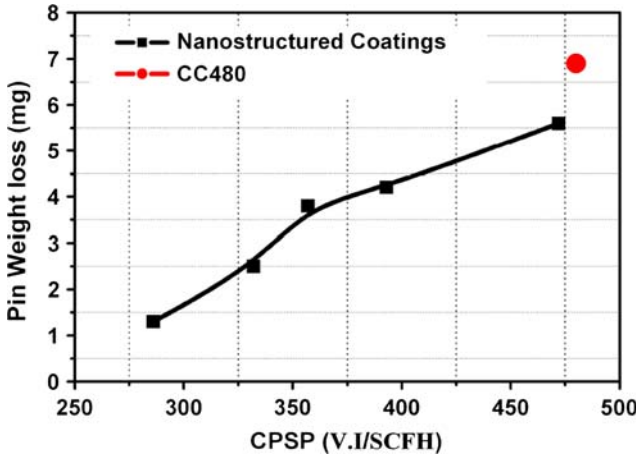

Fig. 13 Pin weight loss vs. CPSP in sliding wear tests

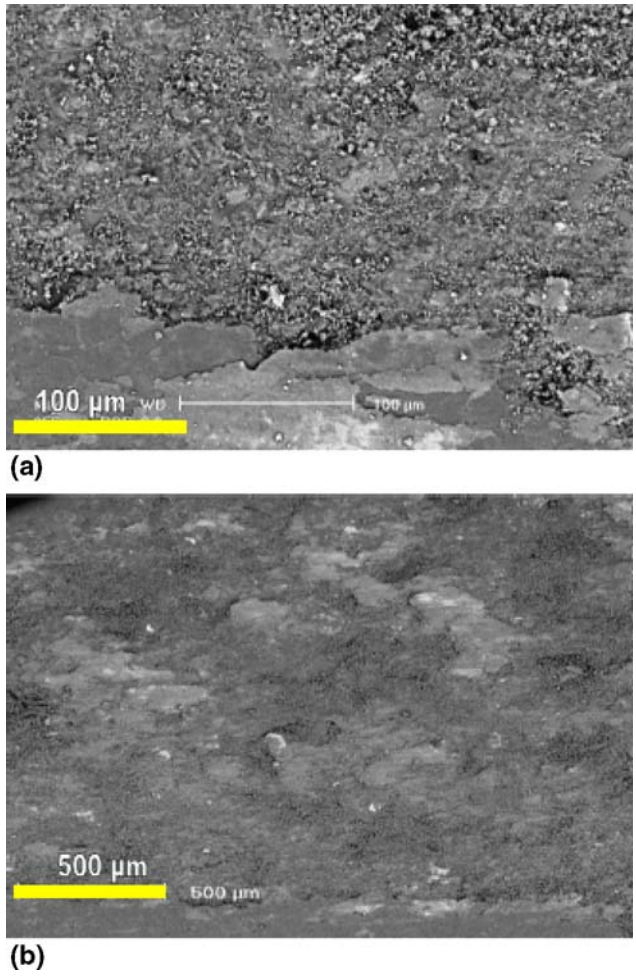

Fig. 14 SEM images of worn surfaces of the conventional and nanostructure coating

cross section experienced numerous small cracks (Fig. 15a), but the cracks in conventional coating growth along the splat boundary and cause the separation of coarse pieces of coating (wear product) during the wear test and initiation and propagation of cracks and delamination of coating due to creation and growth of cracks along the layers boundary.

Since grinding and polishing operations represent about 40% of the total cost of ceramic coating, compared to about 12% for the cost of the feedstock powder, nanostructured coatings are actually less expensive to apply. Thus replacing of conventional coating with the ceramic nanostructured coating cause the reduction of initial cost of coating as compared to conventional Al_2O_3-13% TiO_2 coating because of increasing grindability and decreasing of grinding cost (despite increasing in raw material cost).

Also with regard to fatigue lifetime and wear resistance of nanostructured coatings is higher than the conventional coating, thus nanostructured Al_2O_3-13% TiO_2 coatings longevity is more than conventional casting and using nanostructured Al_2O_3-13% TiO_2 coating leads to cost reduction and cost savings.

4. Conclusions

Based on the findings from the experiments outlined above, the following conclusions can be drawn:

(1) Grindability (material removal rate and quality of ground coatings) of nanostructure Al_2O_3-13% TiO_2 coating is excellent, but conventional coatings have poor grindability.

(2) Fatigue lifetime of nanostructured Al_2O_3-13% TiO_2 coating is about $\times 10$ with respect to conventional coating.

(3) Wear rate of nanostructured Al_2O_3-13% TiO_2 is about a quarter of conventional coating.

(4) Wear rate of nanostructured Al_2O_3-13% TiO_2 coating decrease with an increase in CPSP of plasma spray process.

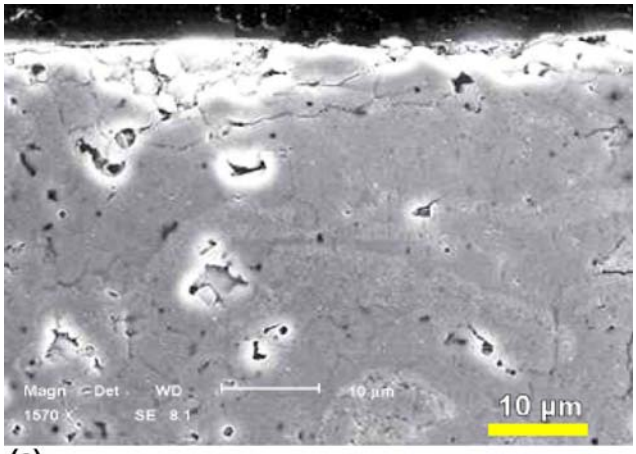

(a)

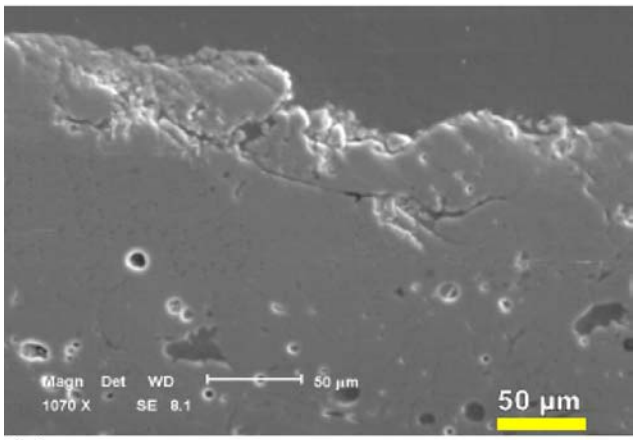

(b)

Fig. 15 SEM images of the worn surfaces cross section of the (a) nanostructure and (b) conventional coatings

(5) Brittle fracture is the basic mechanism in wear of conventional coating, while nanostructured coating worn surface has very smooth features which are the characteristics of wear with plastic deformation mechanism.

(6) The advantages of replacing nanostructure coating with existing conventional ceramic coatings are higher properties, better performance, greater longevity, and reliability.

References

1. R.F. Bunshah, *Handbook of Hard Coatings—Deposition Technologies, Properties and Applications*, Noyes Publications, William Andrew Publishing, LLC, Norwich, NY, USA, ISBN: 0-8155-1438-7
2. Millidyne Surface Technologies, http://www.millidyne.fi/neoxid-powders.html, January 22, 2010
3. Y. Wang, S. Jiang, M. Wang, S. Wang, T.D. Xiao, and P.R. Strutt, Abrasive Wear Characteristics of Plasma Sprayed Nanostructured Alumina/Titania Coatings, *Wear*, 2000, **237**, p 176-185
4. E.H. Jordan, M. Gell, Y.H. Sohn, D. Goberman, L. Shaw, S. Jiang, M. Wang, T.D. Xiao, Y. Wang, and P. Strut, Fabrication and Evaluation of Plasma Sprayed Nanostructured Alumina-Titania Coatings with Superior Properties, *Mater. Sci. Eng.*, 2001, **301**, p 80-89
5. R.S. Lima and B.R. Marple, Thermal Spray Coatings Engineered from Nanostructured Ceramic Agglomerated Powders for Structural, Thermal Barrier and Biomedical Applications: A Review, *J. Therm. Spray Tech.*, 2007, **16**(1), p 40-61
6. L.L. Shaw, D. Goberman, R. Ren, M. Gell, S. Jiang, Y. Wang, T.D. Xia, and P.R. Strutt, The Dependency of Microstructure and Properties of Nanostructured Coatings on Plasma Spray Conditions, *Surf. Coat. Technol.*, 2000, **130**, p 1-8
7. G.E. Kim, Proven and Promising Applications Thermal Sprayed Nanostructured Coatings, *Proceedings of the International Thermal Spray Conference 2006, PDF file in Building on 100 Years of Success: Proceedings of the International Thermal Spray Conference 2006*, B.R. Marple, M.M. Hyland, Y.-C. Lau, R.S. Lima, and J. Voyer, Ed., May 15-18, 2006 (Seattle, WA, USA), ASM International, Materials Park, OH (2006)
8. E.H. Jordan, M. Gell, Y.H. Sohn, D. Goberman, L. Shaw, S. Jiang, M. Wang, T.D. Xiao, Y. Wang, and P. Strutt, Fabrication and Evaluation of Plasma Sprayed Nanostructured Alumina-Titania Coatings with Superior Properties, *Mater. Sci. Eng.*, 2001, **A301**, p 80-89
9. M. Gell, E.H. Jordan, Y.H. Sohn, D. Goberman, L. Shaw, and T.D. Xiao, Development and Implementation of Plasma Sprayed Nanostructured Ceramic Coatings, *Surf. Coat. Technol.*, 2001, **146-147**, p 48-54
10. D. Goberman, Y.H. Sohn, L. Shaw, E. Jordan, and M. Gell, Microstructure Development of Al_2O_3-13 Wt% TiO_2 Plasma Sprayed Coatings Derived from Nanocrystalline Powders, *Acta Mater.*, 2002, **50**, p 1141-1152
11. H. Luo, D. Goberman, L. Shaw, and M. Gell, Indentation Fracture Behavior of Plasma-Sprayed Nanostructured Al_2O_3-13 Wt% TiO_2 Coatings, *Mater. Sci. Eng.*, 2003, **A346**, p 237-245
12. P. Bansal, N.P. Padture, and A. Vasiliev, Improved Interfacial Mechanical Properties of Al_2O_3-13 wt% TiO_2 Plasma-Sprayed Coatings Derived from Nanocrystalline Powders, *Acta Mater.*, 2003, **51**, p 2959-2970
13. M. Ramazani, J. Khalil-Allafi, and R. Mozaffarinia, Fabrication and Evaluation of Nanostructured Plasma Sprayed Al_2O_3-13% TiO_2 Coatings, *9th Iranian National Seminar on Surface Engineering and Heat Treatment*, Iran University of Science and Technology, Iran, 13-14 May 2008
14. G.M. Pharr, Measurement of Mechanical Properties by Indentation, *Mater. Sci. Eng.*, 1998, **A253**, p 151-159
15. J. Ahn, E.P. Song, S. Lee, and N.J. Kim, Wear Resistance of Plasma-Sprayed Al_2O_3-TiO_2 Nanocoatings, *Key Eng. Mater.*, 2007, **345-346**, p 641-644
16. W.M. Rainforth, The Wear Behaviour of Oxide Ceramics—A Review, *J. Mater. Sci.*, 2004, **39**(22), p 6705-6721
17. M. Bounazef, S. Guessasma, G. Monatavon, and C. Coddet, Effect of APS Process Parameters on Wear Behaviour of Alumina-Titania Coatings, *Mater. Lett.*, 2004, **58**, p 2451-2455
18. B. Normand, V. Fervel, and C. Coddet, Tribological Properties of Plasma Sprayed Alumina-Titania Coatings: Role and Control of the Microstructure, *Surf. Coat. Technol.*, 2000, **123**, p 278-283
19. M. Ramazani, J. Khalil-Allafi, and R. Mozaffarinia, *New Material National Congress*, Material and Energy Research Center, Karaj, Iran, 10 June, 2008
20. R.S. Lima and B.R. Marple, Thermal Spray Coatings Engineered from Nanostructured Ceramic Agglomerated Powders for Structural, Thermal Barrier and Biomedical Applications: A Review, *J. Therm. Spray Tech.*, 2007, **16**(1), p 40-63
21. C. Guo and R.H. Chand, Grindability of Ceramics, *Proceeding of the 1st International Machining and Grinding Conference*, SME, MR95-168, Dearborn, MI, p 123-136, 1995
22. C. Guo and R.H. Chand, Grindability and Mechanical Property of Ceramics, *Ceramic Engineering & Science Proceedings*, American Ceramic Society, 1996
23. C. Guo, R.H. Chand, and N. Krishnan, Cost-Effective Method for Determining the Grindability of Ceramics, *Proceedings of the Department of Energy Annual Automotive Technology Development Contractors, Coordination Meeting*, Dearborn, Michigan, 1994
24. Chand Kare Develops Grindability Test System, *Ceram. Technol. Newslett.*, 1995, **47**, 8-9